Journal of Zhejiang University-SCIENCE B (Biomedicine & Biotechnology) 2023 24(6):485-495
www.jzus.zju.edu.cn; www.springer.com/journal/11585
E-mail: jzus_b@zju.edu.cn

Research Article

https://doi.org/10.1631/jzus.B2200562

Fibroblast growth factor 21 (FGF21) attenuates tacrolimus-induced hepatic lipid accumulation through transcription factor EB (TFEB)-regulated lipophagy

Zhensheng ZHANG[1,2,4,5,6*], Li XU[3,4,5,6*], Xun QIU[1,2,4,5,6], Xinyu YANG[1,2,4,5,6], Zhengxing LIAN[1,2,4,5,6], Xuyong WEI[1,2,4,5,6], Di LU[1,2,4,5,6], Xiao XU[1,2,4,5,6✉]

[1]*Zhejiang University School of Medicine, Hangzhou 310058, China*
[2]*Key Laboratory of Integrated Oncology and Intelligent Medicine of Zhejiang Province, Hangzhou 310006, China*
[3]*Department of Hepatobiliary and Pancreatic Surgery, the First Affiliated Hospital, Zhejiang University School of Medicine, Hangzhou 310003, China*
[4]*Institute of Organ Transplantation, Zhejiang University, Hangzhou 310003, China*
[5]*NHC Key Laboratory of Combined Multi-organ Transplantation, Hangzhou 310003, China*
[6]*Westlake Laboratory of Life Sciences and Biomedicine, Hangzhou 310024, China*

Abstract: Tacrolimus (TAC), also called FK506, is one of the classical immunosuppressants to prevent allograft rejection after liver transplantation. However, it has been proved to be associated with post-transplant hyperlipemia. The mechanism behind this is unknown, and it is urgent to explore preventive strategies for hyperlipemia after transplantation. Therefore, we established a hyperlipemia mouse model to investigate the mechanism, by injecting TAC intraperitoneally for eight weeks. After TAC treatment, the mice developed hyperlipemia (manifested as elevated triglyceride (TG) and low-density lipoprotein cholesterol (LDL-c), as well as decreased high-density lipoprotein cholesterol (HDL-c)). Accumulation of lipid droplets was observed in the liver. In addition to lipid accumulation, TAC induced inhibition of the autophagy-lysosome pathway (microtubule-associated protein 1 light chain 3β (LC3B) II/I and LC3B II/actin ratios, transcription factor EB (TFEB), protein 62 (P62), and lysosomal-associated membrane protein 1 (LAMP1)) and downregulation of fibroblast growth factor 21 (FGF21) in vivo. Overexpression of FGF21 may reverse TAC-induced TG accumulation. In this mouse model, the recombinant FGF21 protein ameliorated hepatic lipid accumulation and hyperlipemia through repair of the autophagy-lysosome pathway. We conclude that TAC downregulates FGF21 and thus exacerbates lipid accumulation by impairing the autophagy-lysosome pathway. Recombinant FGF21 protein treatment could therefore reverse TAC-caused lipid accumulation and hypertriglyceridemia by enhancing autophagy.

Key words: Autophagy; Fibroblast growth factor 21 (FGF21); Lipid; Lipophagy; Lysosome; Tacrolimus; Transcription factor EB (TFEB)

1 Introduction

Liver transplantation is the most effective method for treating end-stage liver disease and early-stage liver cancer. For optimal outcomes, liver-transplant recipients usually need to take immunosuppressive agents. One of the most-used drugs is tacrolimus (TAC), also called FK506. It belongs to the calcineurin inhibitors, and attenuates allograft rejection by inhibiting T-cell function (Choi and Reddy, 2014). However, application of these immunosuppressive agents often results in metabolic disorders. For example, TAC plays a significant role in dyslipidemia (Dehghani et al., 2007; Rostaing et al., 2012), which is a non-negligible risk factor for cardiovascular events (Ryan et al., 2018). Therefore, alleviating the dyslipidemia caused by TAC is key to improving quality of life for liver transplant recipients.

Lipids can be degraded by autophagy, which contributes to maintaining the balance of lipid metabolism; lipophagy is a selective autophagy that targets lipid droplets (Zhang T et al., 2020). Autophagy is

✉ Xiao XU, zjxu@zju.edu.cn
* The two authors contributed equally to this work
Xiao XU, https://orcid.org/0000-0002-2761-2811

Received Nov. 3, 2022; Revision accepted Feb. 19, 2023;
Crosschecked May 16, 2023

a highly conserved intracellular degradative process. There are three main forms of autophagy: macroautophagy, chaperone-mediated autophagy, and microautophagy (Wang SY et al., 2022). During the process, unneeded cytoplasmic components are packed into double-membrane vesicles known as autophagosomes and delivered to the lysosomes for degradation. Transcription factor EB (TFEB) is one of the master regulators that control autophagy and lysosome biogenesis (Settembre et al., 2011). It is located predominantly in the cytoplasm, but a number of conditions such as infection and mitochondrial damage affect TFEB nuclear translocation and regulate autophagy (Visvikis et al., 2014; Nezich et al., 2015). TFEB regulates multiple genes involved in autophagosome biogenesis, autophagosome-lysosome fusion, and lysosomal degradation pathways (Ballabio and Bonifacino, 2020). Therefore, whether TFEB-regulated autophagy participates in TAC-induced lipid accumulation is a worthwhile question to pursue.

Fibroblast growth factor 21 (FGF21) is an endocrine member of the FGF family and has been linked with autophagy (Byun et al., 2020; Qiang et al., 2021). It is abundantly secreted by the liver, which produces more than 80% of the total circulating FGF21 (Hondares et al., 2011). A series of environmental conditions, such as starvation and exercise, can induce FGF21 expression (Inagaki et al., 2007; Sui and Chen, 2022). It appears to participate in maintaining glucose and lipid homeostasis (Geng et al., 2020). However, the mechanism by which FGF21 takes part in these processes is unclear. Also, whether FGF21 plays a role in immunosuppressor-induced metabolic disorders is still unknown.

In the present study, we investigated the role of FGF21 in TAC-induced hepatic lipid accumulation in vivo and in vitro.

2 Materials and methods

2.1 Chemicals and reagents

Recombinant human FGF21 (rhFGF21, CM110) was purchased from Chamot Biotechnology Co., Ltd. (Shanghai, China). Recombinant mouse FGF21 (rmFGF21, Z03290) was purchased from GenScript (New Jersey, USA). TAC (S5003) was purchased from Selleck (Shanghai, China). A total RNA purification kit (19221ES) and first strand complementary DNA (cDNA) synthesis kit (11142ES) were purchased from Yeason (Shanghai, China). A mouse FGF21 enzyme-linked immunosorbent assay (ELISA) kit (ab212160) was purchased from Abcam (Cambridge, UK). Oil Red O (ORO) solution (G1260) was purchased from Beijing Solarbio Science & Technology Co., Ltd. (Beijing, China). SYBR green quantitative real-time polymerase chain reaction (qPCR) Master Mix (Q431-02) was purchased from Vazyme (Nanjing, China). A hematoxylin-eosin (HE) staining kit (C0105S) and nuclear and cytoplasmic protein extraction kit (P0027) were purchased from Beyotime (Shanghai, China). Triglyceride (TG, A110-1-1), total cholesterol (TC, A111-1-1), high-density lipoprotein cholesterol (HDL-c, A112-1-1), and low-density lipoprotein cholesterol (LDL-c, A113-1-1) quantification kits were purchased from Nanjing Jiancheng Bioengineering Institute (Nanjing, China).

2.2 Animal model

Eight-week-old C57BL/6J male mice were obtained from the Zhejiang Academy of Medical Sciences and housed in cages at 20 ℃ under a 12-h light/dark cycle. Mice were fed a normal chow diet. To evaluate the effect of TAC on lipid metabolism, mice were randomly divided into two groups with equal body weight: (1) mice intraperitoneally injected daily with solvent (NC group); and (2) mice intraperitoneally injected daily with TAC (1 mg/(kg·d)) (TAC group). Administration lasted for eight weeks. The solvent was composed as follows (volume fraction): 2% dimethyl sulfoxide (DMSO)+40% poly ethylene glycol 300 (PEG300)+5% Tween 80+53% deionized H_2O (ddH_2O). To evaluate the effect of rmFGF21, after eight weeks, mice treated with TAC were injected daily with TAC and rmFGF21 (1 mg/(kg·d)) for two weeks. Body weight was regularly recorded every two weeks. Finally, after the mice were sacrificed, the serum lipid profiles (TG, TC, HDL-c, and LDL-c) were detected.

2.3 Cell culture and treatment

HepG2 and AML12 cell lines were purchased from the Cell Bank of the Chinese Academy of Sciences (Shanghai, China). The HepLi-2 cell line was obtained from Zhejiang University (Hangzhou, China). HepG2 and HepLi-2 cells were maintained in Dulbecco's modified Eagle's medium (DMEM; Gibco, USA) supplemented with 10% (volume fraction) fetal bovine serum

(FBS). AML12 cells were maintained in DMEM/F12 medium (Sigma, USA) containing 10 μg/mL insulin, 5.5 μg/mL transferrin, 5 ng/mL selenium, 40 ng/mL dexamethasone, and 10% FBS. All cell lines were kept at 37 ℃ in a humidified atmosphere of 95% air with 5% CO_2.

For TAC treatment, cells were treated with 20 ng/mL TAC or DMSO as control for 48 h. To evaluate the effect of recombinant FGF21 protein, cells were co-treated with TAC and the protein for 48 h. To assess FGF21 overexpression, HepG2, HepLi-2, and AML12 cells were transfected with the overexpression plasmid (GenePharma, Shanghai, China) using Lipo3000 transfection reagent (Invitrogen, USA) and following the manufacturer's protocol.

After the treatments, cells were harvested to detect the TG content, following the manufacturer's protocol.

2.4 Western blot analysis and immunostaining

Antibodies were purchased from the following sources: anti-FGF21 (ab171941) and anti-protein 62 (anti-P62, ab109012) from Abcam; anti-microtubule-associated protein 1 light chain 3β (anti-LC3B, CY5992) from Abways Biotechnology Co., Ltd. (Shanghai, China); anti-histone H3 (17168-1-AP) and anti-lysosomal-associated membrane protein 1 (anti-LAMP1, 55273-1-AP) from Proteintech (Wuhan, China); and anti-actin (AC026) from Abclonal (Wuhan, China). For immunofluorescence analysis, anti-LC3B (98557) was purchased from Cell Signaling Technology (Massachusetts, USA). Anti-LAMP1 (CL647-65050 and CL647-65051) was purchased from Proteintech and Lipi-Red was purchased from Dojindo Molecular Technologies, Inc. (Japan), for fluorescence staining of lipid droplets.

Mouse livers were dissected and fixed with buffered 4% (volume fraction) paraformaldehyde (PFA) overnight, then cryoprotected in 30% (0.3 g/mL) sucrose solution overnight, and finally embedded in optimal cutting temperature (OCT) compound (Biosharp, Hefei, China). HepG2 and AML12 cell lines were fixed in 4% PFA for 10 min. For immunostaining, cells or cryostat sections (7 μm) were permeabilized in 0.5% (5 g/L) Triton X-100 for 5 min and blocked in 5% (0.05 g/mL) bull serum albumin (BSA) for 1 h, and then incubated with the appropriate antibodies or Lipi-Red.

2.5 qPCR

Total RNA was extracted from cells and mouse livers using the total RNA purification kit, and cDNA was obtained with the first strand cDNA synthesis kit, following the manufacturer's protocol. qPCR was performed on a CFX96 Touch real-time PCR system (Bio-Rad, California, USA) with the SYBR green qPCR Master Mix. The primers used for qPCR were listed in Table S1.

2.6 ORO staining

Lipid staining of cultured cells and mouse-liver tissue was performed using ORO solution, following the manufacturer's protocol. Cells were cultured on glass coverslips in a 6-well plate and then fixed with 4% PFA at room temperature for 15 min. Next, cells were rinsed with phosphate-buffered solution (PBS) and incubated with ORO reagent at room temperature for 15 min. Then, the ORO reagent was removed and the coverslips were washed with distilled water. Finally, the nuclei were stained with hematoxylin. To stain the tissue, each frozen left liver lobe was cut into 4-μm slices and affixed to microscope slides. The remaining steps were as described above.

2.7 HE staining

For tissue histology, mouse liver tissues were fixed in 4% PFA overnight and embedded in paraffin. Then they were cut into 7-μm slices and dyed using the HE staining kit, following the manufacturer's protocol.

2.8 Statistical analysis

All assays were repeated at least three times. Data are presented as the mean±standard deviation (SD) and were analyzed using GraphPad Prism 8 (Dotmatics, California, USA). Differences between groups were determined using Student's *t*-tests or one-way analysis of variance (ANOVA). Values of $P<0.05$ were considered to be significantly different.

3 Results

3.1 Induction of hepatic lipid accumulation and hypertriglyceridemia by TAC

Since TAC treatment often brings about hyperlipemia in liver transplant recipients (Dehghani et al., 2007), we first explored the role of TAC in lipid metabolism. In the liver sections of the mouse model described above, the accumulation of lipid droplets was obvious in the TAC group by ORO and HE staining (Figs. 1a

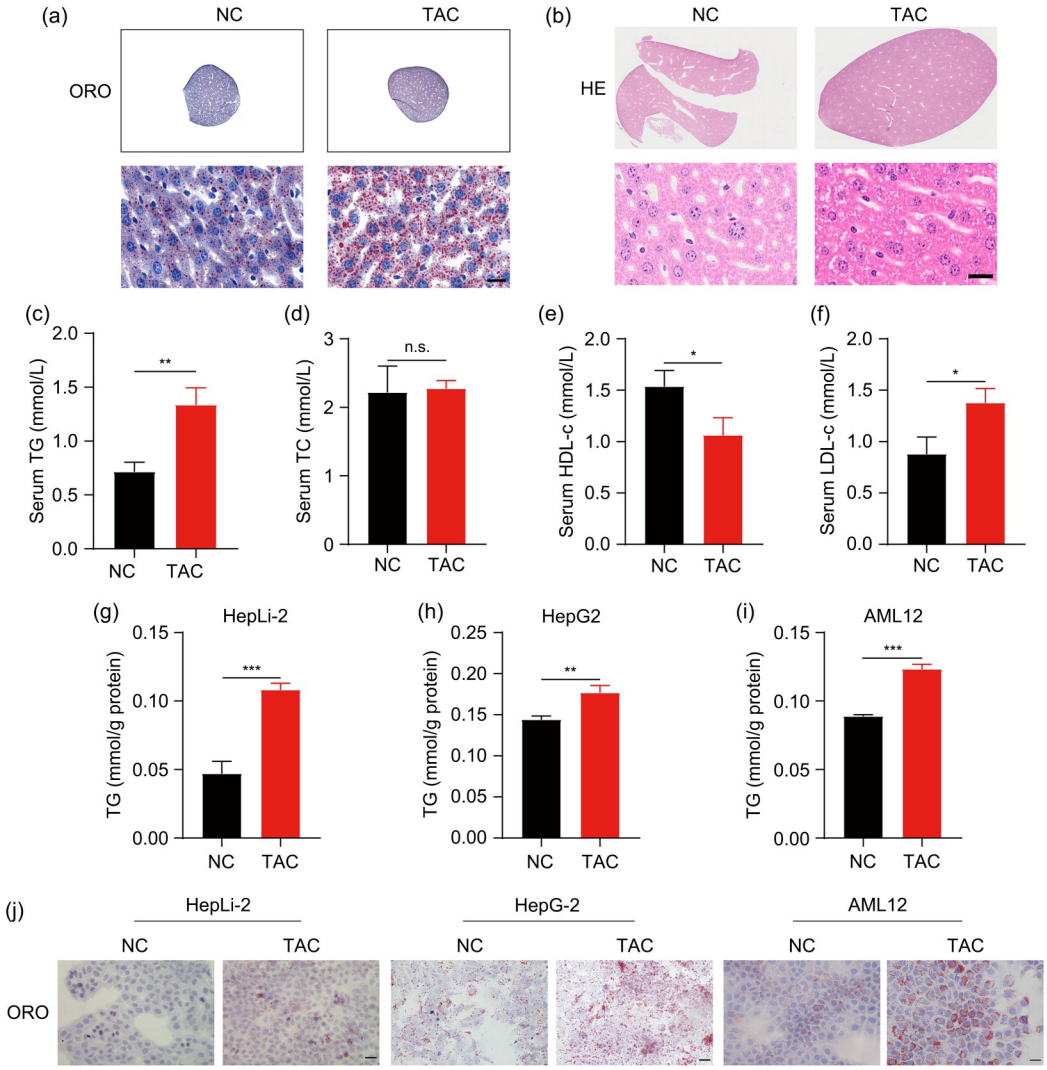

Fig. 1 Induction of hepatic lipid accumulation and hypertriglyceridemia by TAC. (a, b) Representative ORO and HE staining results of liver sections after TAC treatment for eight weeks. (c–f) TG, TC, HDL-c, and LDL-c levels in mouse plasma. (g–i) TG contents of the three cell lines (HepLi-2, HepG2, and AML12) after TAC treatment for 48 h. (j) Representative ORO staining results of the three cell lines. Scale bar=20 μm. Data are shown as mean±SD, n=3. * P<0.05, ** P<0.01, *** P<0.001; n.s.: not significant. HE: hematoxylin-eosin; ORO: Oil Red O; TAC: tacrolimus; NC: negative control; TC: total cholesterol; TG: triglyceride; LDL-c: low-density lipoprotein cholesterol; HDL-c: high-density lipoprotein cholesterol; SD: standard deviation.

and 1b). Then we detected the routine clinical parameters of lipid in serum. The levels of TG and LDL-c increased, while HDL-c decreased after TAC treatment, which corresponded to a sign of hyperlipemia (Figs. 1c, 1e, and 1f). However, serum levels of TC were similar in the NC and TAC groups, indicating that TAC mainly resulted in hypertriglyceridemia (Fig. 1d). There was no significant difference in weight between the two groups (Fig. S1). Then, we explored the effects of TAC in three hepatic cell lines (HepG2, HepLi-2, and AML12). Consistent with the results of in vivo study, TAC led to a significant accumulation of TG and lipid droplets compared with the control (Figs. 1g–1j).

3.2 Induction of lipid accumulation by TAC through inhibition of the TFEB-mediated autophagy-lysosome pathway

We attributed homeostasis of the lipid metabolism to an equilibrium between synthesis and consumption. Based on the intimate association between autophagy and lipid homeostasis, we evaluated the markers of the autophagy-lysosome pathway, including LC3B,

LAMP1, P62, and TFEB. Because HepLi-2 and AML12 cells are both normal hepatic cell lines and their phenotypes were similar, we chose AML12 and HepG2 cells for exploration of the autophagy-lysosome pathway. LC3B is the most commonly employed autophagosome marker (Klionsky et al., 2021). In response to TAC treatment, HepG2 and AML12 cells exhibited reduced LC3B II/I and LC3B II/actin ratios, indicating inactivation of autophagy (Fig. 2a). The messenger RNA (mRNA) level of LC3B did not change after TAC treatment (Fig. S2). P62 is another marker for autophagy flux and it was increased after TAC treatment, indicating that autophagy flux was blocked (Fig. 2a). TFEB is a switch of the autophagy-lysosome pathway. We found that TAC treatment not only prevented import of TFEB to the nucleus, but also reduced expression of TFEB (Fig. 2a). Moreover, our results indicated that expression of LAMP1 was downregulated, suggesting a reduction in lysosomes caused by treatment with TAC (Fig. 2a). Immunofluorescence analysis showed impaired total expression and nuclear localization of TFEB induced by TAC (Fig. 2b). In addition, TAC treatment appeared to reduce autophagosomes as LC3B punctae were reduced (Fig. 2c). Consistently, decreased colocalization of LAMP1 and lipid droplets demonstrated that fewer lipid droplets were degraded through the autophagy-lysosome pathway in the TAC group (Fig. 2d). Thus, our results showed that TAC damaged the autophagy-lysosome pathway and stored up the lipids.

3.3 Reversion of TAC-induced lipid accumulation by overexpression of FGF21

FGF21 plays a vital role in regulating the lipid metabolic process (Geng et al., 2020). Therefore, we wanted to find out whether TAC would affect FGF21 expression. As we expected, the protein and mRNA levels of FGF21 both appeared to be downregulated in the TAC group (Figs. 3a and 3b). Given that FGF21 is a secreted protein, we measured the serum level of

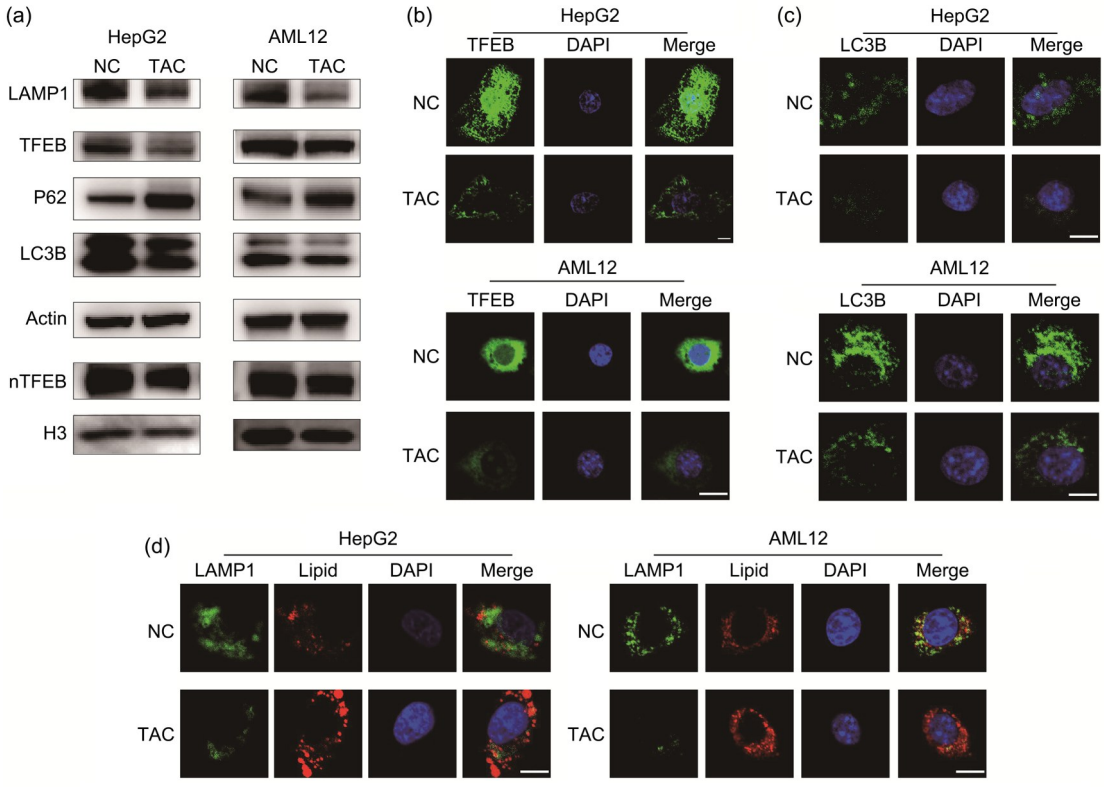

Fig. 2 Induction of lipid accumulation by TAC through autophagy inhibition. (a) Immunoblot detection of LAMP1, TFEB, P62, LC3B, and nTFEB in HepG2 and AML12 cell lines. (b) Representative TFEB staining results of the two cell lines. (c) Representative LC3B staining results of the two cell lines. (d) Representative LAMP1 and lipid-droplet staining results of the two cell lines. Scale bar=10 μm. TAC: tacrolimus; NC: negative control; LAMP1: lysosomal-associated membrane protein 1; TFEB: transcription factor EB; P62: protein 62; LC3B: microtubule-associated protein 1 light chain 3β; nTFEB: nuclear TFEB; H3: histone 3; DAPI: 4',6-diamidino-2-phenylindole.

FGF21 in mice. The results indicated that the serum FGF21 levels were lower in TAC-treated mice than in the control (Fig. 3c). In vitro examination also verified TAC-induced reduction of FGF21 in the three hepatic cell lines (Figs. 3d and 3e). To investigate the role of FGF21 in TAC-induced lipid accumulation, we used a plasmid-based approach to overexpress FGF21. As evidenced by immunoblot and qPCR, FGF21 was successfully overexpressed in three cell lines (Figs. 3f and 3g). We found that TG accumulation caused by TAC was attenuated in FGF21-overexpressing cells (Fig. 3h). ORO staining also indicated a reduction in lipid droplets in FGF21-overexpressed cells compared with TAC-treated cells (Fig. 3i). These results suggested the important role of FGF21 in maintaining lipid homeostasis under TAC treatment.

3.4 Reversion of TAC-induced lipid accumulation and hypertriglyceridemia by recombinant FGF21 protein

FGF21 is a secreted protein, which means that it has the capacity to regulate lipid homeostasis throughout the body (Hondares et al., 2011). After discovering that overexpression of FGF21 could ameliorate lipid

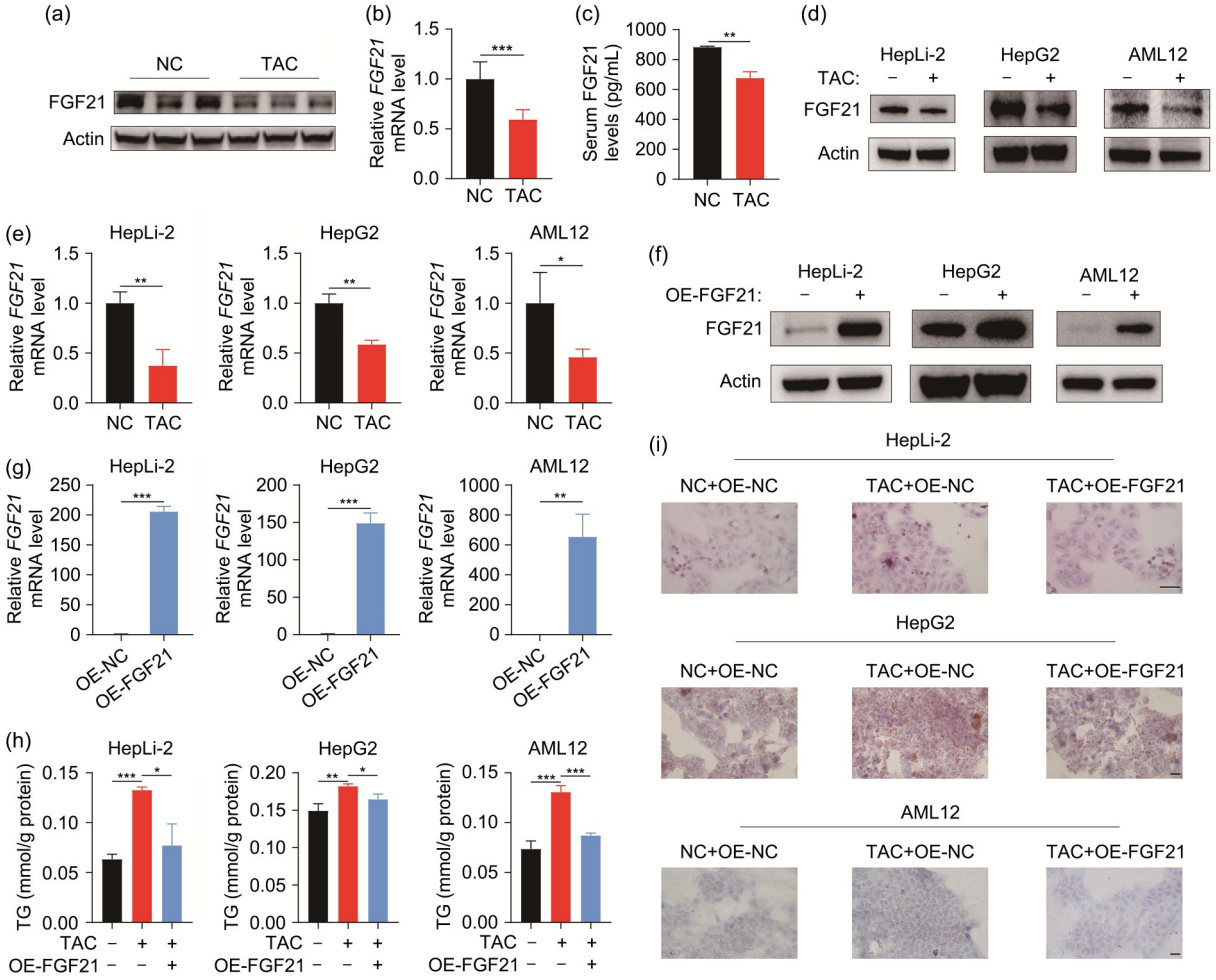

Fig. 3 Reversion of TAC-induced lipid accumulation by overexpression of FGF21. (a) Immunoblot detection of FGF21 expression in the liver. (b) qPCR-assisted detection of FGF21 in the liver. (c) FGF21 serum level. (d) Immunoblot detection of FGF21 expression in three cell lines. (e) qPCR-assisted detection of FGF21 in three cell lines. (f) Immunoblot detection of FGF21 overexpression in three cell lines. (g) qPCR-assisted detection of FGF21 overexpression in three cell lines. (h) TG contents after DMSO or TAC treatment in three cell lines with or without FGF21 overexpression. (i) Representative ORO staining results of three cell lines. Scale bar=20 μm. Data are shown as mean±SD, n=3. * P<0.05, ** P<0.01, *** P<0.001. ORO: Oil Red O; FGF21: fibroblast growth factor 21; TAC: tacrolimus; NC: negative control; OE: overexpression; qPCR: quantitative real-time polymerase chain reaction; TG: triglyceride; DMSO: dimethyl sulfoxide; mRNA: messenger RNA; SD: standard deviation.

packing in cell lines caused by TAC, we attempted to determine the efficacy of recombinant FGF21 protein in the treatment of TAC-induced hyperlipemia. The experimental process of in vivo study is shown in Fig. 4a. ORO and HE staining showed that lipid-droplet accumulation caused by TAC treatment was decreased by rmFGF21 in mouse livers (Fig. 4b). Despite the reduction in serum TG level in mice that received rmFGF21 (Fig. 4c), there were no significant effects of rmFGF21 in terms of reversing altered HDL-c or LDL-c level induced by TAC (Figs. 4d and 4e). In HepG2 and AML12 cells, lipid-droplet storage and TG accumulation triggered by TAC were also eliminated after recombinant FGF21 protein treatment (Figs. 4f and 4g).

3.5 Effect of recombinant FGF21 protein on the TFEB-regulated autophagy-lysosome pathway impaired by TAC

Because FGF21 has been proved to be associated with the autophagy-lysosome pathway and TAC suppressed it, as we mentioned above (Byun et al., 2020), we assumed that the attenuation of TAC-induced lipid accumulation resulting from recombinant FGF21 protein treatment was promoted by repair of this pathway. Compared with TAC treatment, western blot analysis showed that rmFGF21 administration reversed the downregulation of TFEB, LAMP1, LC3B II/I ratio, and LC3B II/actin ratio caused by TAC (Fig. 5a). Nuclear transport of TFEB also increased in mice treated with

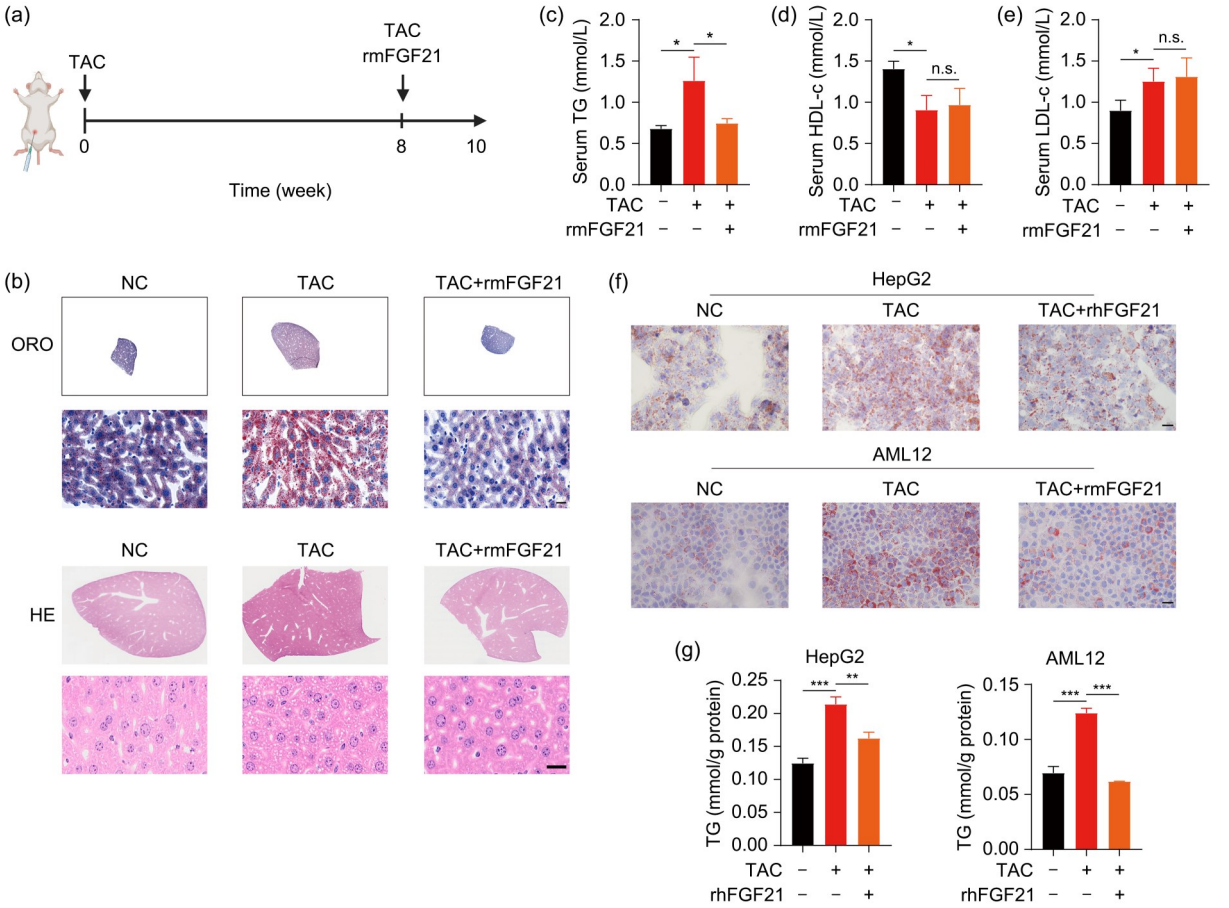

Fig. 4 Reversion of defective lipid homeostasis by recombinant FGF21 protein. (a) The experimental process of in vivo study. (b) Representative ORO and HE staining results of liver sections after co-treatment with TAC and recombinant FGF21 protein. (c–e) TG, HDL-c, and LDL-c levels in mouse plasma. (f) Representative ORO staining results in HepG2 and AML12 cells after TAC treatment for 48 h with or without recombinant FGF21 co-treatment. (g) TG contents in HepG2 and AML12 cells. Scale bar=20 μm. Data are shown as mean±SD, n=3. * P<0.05, ** P<0.01, *** P<0.001; n.s.: not significant. FGF21: fibroblast growth factor 21; ORO: Oil Red O; HE: hematoxylin-eosin; TAC: tacrolimus; NC: negative control; TG: triglyceride; LDL-c: low-density lipoprotein cholesterol; HDL-c: high-density lipoprotein cholesterol; rmFGF21: recombinant mouse FGF21; SD: standard deviation.

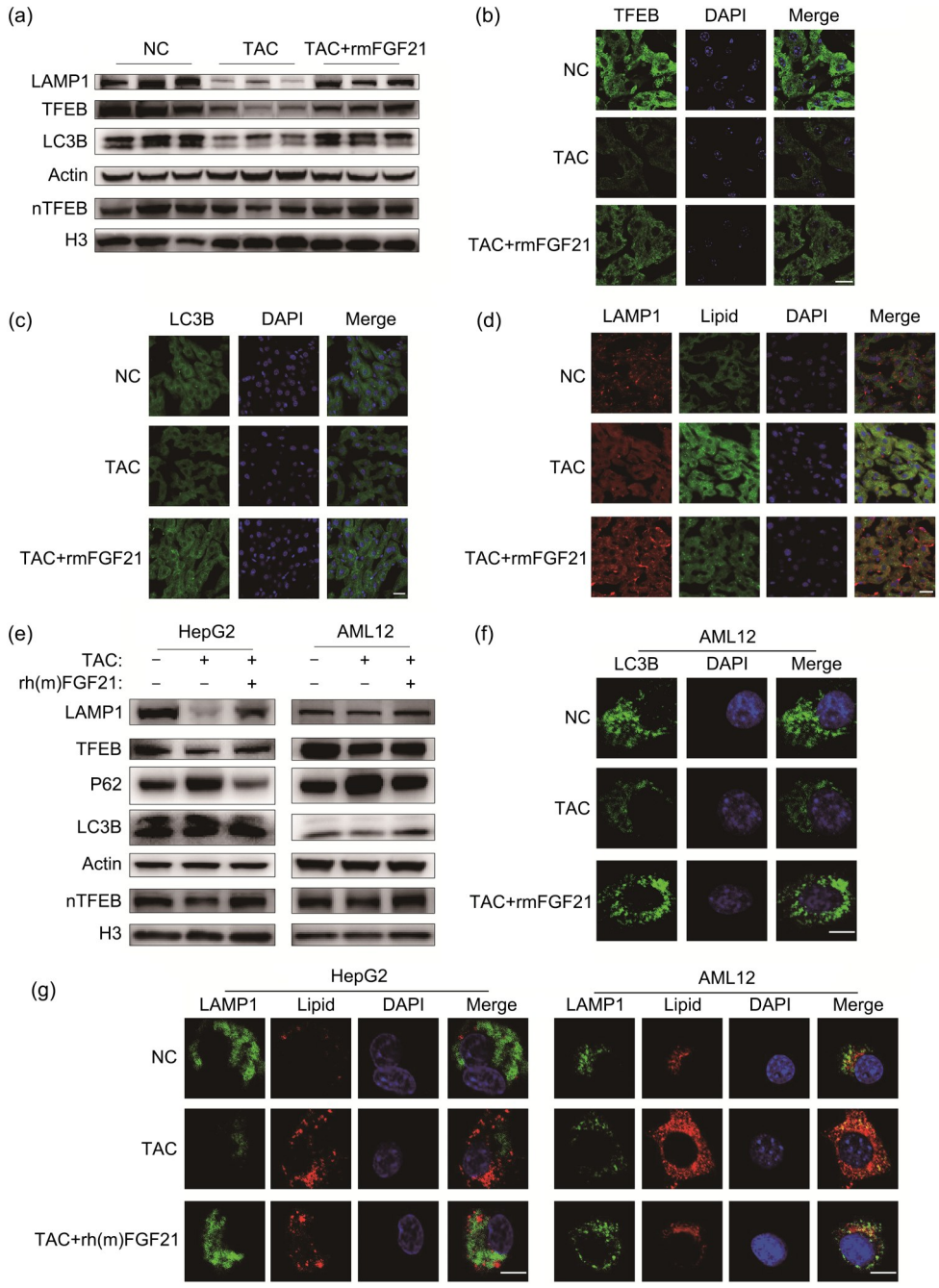

Fig. 5 Effect of recombinant FGF21 protein on TAC-impaired autophagy. (a) Immunoblot detection of LAMP1, TFEB, P62, LC3B, and nTFEB in mouse livers. (b) Representative TFEB staining results of liver sections. (c) Representative LC3B staining results of liver sections. (d) Representative LAMP1 and lipid-droplet staining results of liver sections. (e) Immunoblot detection of LAMP1, TFEB, LC3B, and nTFEB in HepG2 and AML12 cell lines. (f) Representative LC3B staining results of AML12 cell line. (g) Representative LAMP1 and lipid-droplet staining results of the two cell lines. Scale bar=10 μm. FGF21: fibroblast growth factor 21; LAMP1: lysosomal associated membrane protein 1; TFEB: transcription factor EB; P62: protein 62; LC3B: microtubule-associated protein 1 light chain 3β; TAC: tacrolimus; NC: negative control; nTFEB: nuclear TFEB; rh(m)FGF21: recombinant human (mouse) FGF21; DAPI: 4',6-diamidino-2-phenylindole; H3: histone 3.

TAC and rmFGF21, compared with that in mice treated with TAC alone (Figs. 5a and 5b). Corresponding to these observations, the increase in LC3B punctae, enhanced colocalization of LAMP1, and accumulation of lipid droplets collectively indicated that rmFGF21 decreased TAC-induced hepatic lipid accumulation

through the autophagy-lysosome pathway (Figs. 5c and 5d). Compared with those treated with TAC alone, cells additionally treated with recombinant FGF21 protein exhibited higher expression of TFEB and LAMP1 proteins (Fig. 5e). Both the LC3B II/I ratio and LC3B II/actin ratio were upregulated, while P62 was downregulated; nuclear transport of TFEB was enhanced as well (Fig. 5e). Immunofluorescence results demonstrated that the combined application promoted production of LC3B punctae, indicating the reversion of TAC-caused impairment of the autophagy-lysosome pathway (Fig. 5f). The observation that colocalization of LAMP1 and lipid droplets was facilitated further clarified that recombinant FGF21 protein attenuated TAC-induced lipid accumulation by boosting the autophagy-lysosome pathway (Fig. 5g).

4 Discussion

Immunosuppressive agents are an indispensable treatment method for transplant recipients to reduce rejection. However, the complications which accompany their use are also nonnegligible. Dyslipidemia is one of the more common complications, and is very likely to trigger cardiovascular disease (Achila et al., 2022). Nevertheless, the underlying mechanisms of immunosuppressor-induced dyslipidemia remain to be clarified. Lipid homeostasis consists of two processes: synthesis and decomposition. Our previous study showed that in mice, TAC caused dysregulation of hepatic TG homeostasis through the circular fatty acid synthase (circFASN)/microRNA-33a (miR-33a) pathway (Zhang CZ et al., 2020). This pathway then upregulated stimulating sterol regulatory element-binding protein (SREBP) and FASN, two key lipogenic enzymes that participate in de novo fatty acid synthesis (Zhang CZ et al., 2020). Another study also demonstrated that TAC upregulates stimulating SREBP1 in vivo and in vitro (Ling et al., 2020). Therefore, we attempted to explore whether the decomposition of lipids was affected by TAC. We found that indeed, TAC inhibits lipophagy.

Downregulated serum HDL-c and upregulated serum LDL-c levels are observable in mice treated with TAC. Therefore, we surmised that dyslipidemia was triggered by increased lipid export from hepatocytes. Interestingly, the serum TC level is not significantly changed after TAC treatment. However, we did not measure the TC content in hepatocytes in vivo or in vitro, which is a deficiency of the study. Adipose tissue is another tissue closely linked to lipid homeostasis. Thus, it is an intriguing enigma whether adipose tissue plays a role in TAC-induced dyslipidemia. Interestingly, Pereira et al. (2013) found that TAC can enhance the lipolysis rate and decrease the insulin-stimulated lipogenesis rate in human adipose tissue.

The liver is the main organ that produces and secrets FGF21 (Markan et al., 2014), which is considered a powerful regulator for controlling metabolism homeostasis (She et al., 2022). However, whether FGF21 can directly affect hepatocytes is still unknown due to the low expression of the major receptor FGFR1 in liver tissue (Kurosu et al., 2007). Nevertheless, other studies have offered opposite opinions, claiming that hepatocytes are the target cells of FGF21 (Chen et al., 2017; Wu et al., 2021). Our current study suggests that FGF21 can directly regulate the lipid metabolism of hepatocytes, and that overexpression of FGF21 reduces TAC-induced TG accumulation. Although recombinant FGF21 protein has a similar effect and limits elevation of serum TG levels, it fails to rectify TAC-induced LDL-c and HDL-c disorders. Therefore, we venture to suppose that recombinant FGF21 protein mainly regulates TG homeostasis, most likely because FGF21 plays an indispensable role in lipid degradation and fatty acid oxidation, and TG is one of the most suitable substrates to provide fatty acids (Fisher and Maratos-Flier, 2016).

Autophagy is a crucial way to remove the components which cells do not urgently need. Previous studies have shown the prominent role of the autophagy-lysosome pathway in lipid degradation (Qin et al., 2022; Wang YH et al., 2022). However, whether TAC-induced lipid accumulation is a consequence of autophagy inhibition is undetermined. TAC is a calcineurin inhibitor that regulates cytoplasmic calcium, which is an important factor in autophagy (Medina, 2021). Therefore, we assumed that TAC might affect the autophagy process, and the results were exactly as we expected. In addition, we found that recombinant FGF21 protein is capable of reinforcing autophagy even under TAC treatment, though the latent mechanisms are still obscure. Previous studies have found that FGF21 regulates lipophagy through downstream regulatory element antagonist modulator (DREAM)-protein phosphatase 2 catalytic subunit α (PPP2CA)-regulated TFEB (Tao

et al., 2022). Also, TFEB has been found to be a direct target of forkhead box O1 (FoxO1) (Liu et al., 2016). The exact signaling pathway which TAC regulates thus needs to be further explored. Rapamycin is another immunosuppressive agent known as a mammalian target of rapamycin (mTOR) inhibitor. mTOR is a key molecule in nutrient metabolism and autophagy procedure (Li et al., 2021; Yan et al., 2022). Although some studies have proved that rapamycin confines lipid accumulation by enhancing autophagy, rapamycin surprisingly causes clinical indicators of hyperlipemia, signifying that there are other interference factors that cause the lipid disorder in patients taking rapamycin (Veroux et al., 2011; Liu et al., 2022).

Altogether, our results reveal that TAC downregulates FGF21 to provoke hepatic lipid accumulation and hypertriglyceridemia by discouraging the autophagy-lysosome pathway, and that recombinant FGF21 protein is able to promote lipid degradation by mitigating the autophagy suppression caused by TAC.

5 Conclusions

In summary, we demonstrated that TAC triggers FGF21 downregulation and hepatic TG accumulation resulting from inhibition of lipid degradation through the autophagy-lysosome pathway, and causes hyperlipemia. Overexpression of FGF21 could alleviate TG accumulation induced by TAC. Moreover, recombinant FGF21 protein could reverse suppression of lipophagy, thereby eliminating TAC-induced hepatic TG accumulation and hypertriglyceridemia.

Acknowledgments

This work was supported by the National Key Research and Development Program of China (No. 2021YFA1100500), the National Natural Science Foundation of China (Nos. 92159202, 81930016, and 82102910), the Key Research & Development Plan of Zhejiang Province (No. 2019C03050), the Construction Fund of Key Medical Disciplines of Hangzhou (No. OO20200093), the Postdoctoral Science Foundation (No. 2020M671762), and the Medical and Health Technology Program in Zhejiang Province (No. WKJ-ZJ-2120), China.

Author contributions

Zhensheng ZHANG, Li XU, Xun QIU, and Xiao XU designed the research. Zhensheng ZHANG, Li XU, Xun QIU, Xinyu YANG, and Zhengxing LIAN performed experiments. Zhensheng ZHANG, Li XU, and Xun QIU analyzed and interpreted data. Zhensheng ZHANG wrote the paper. Li XU, Xun QIU, Xuyong WEI, Di LU, and Xiao XU critically reviewed the manuscript. All authors have read and approved the final manuscript, and therefore, have full access to all the data in the study and take responsibility for the integrity and security of the data.

Compliance with ethics guidelines

Zhensheng ZHANG, Li XU, Xun QIU, Xinyu YANG, Zhengxing LIAN, Xuyong WEI, Di LU, and Xiao XU declare no competing interests.

All animal studies were approved by the Institutional Animal Care and Use Committee and the Ethics Committee of Zhejiang University (No. 1482).

References

Achila OO, Fessahye N, Mengistu ST, et al., 2022. A community based cross sectional study on the prevalence of dyslipidemias and 10 years cardiovascular risk scores in adults in Asmara, Eritrea. *Sci Rep*, 12:5567. https://doi.org/10.1038/s41598-022-09446-9

Ballabio A, Bonifacino JS, 2020. Lysosomes as dynamic regulators of cell and organismal homeostasis. *Nat Rev Mol Cell Biol*, 21(2):101-118. https://doi.org/10.1038/s41580-019-0185-4

Byun S, Seok S, Kim YC, et al., 2020. Fasting-induced FGF21 signaling activates hepatic autophagy and lipid degradation via JMJD3 histone demethylase. *Nat Commun*, 11:807. https://doi.org/10.1038/s41467-020-14384-z

Chen LQ, Wang K, Long AJ, et al., 2017. Fasting-induced hormonal regulation of lysosomal function. *Cell Res*, 27(6): 748-763. https://doi.org/10.1038/cr.2017.45

Choi SW, Reddy P, 2014. Current and emerging strategies for the prevention of graft-versus-host disease. *Nat Rev Clin Oncol*, 11(9):536-547. https://doi.org/10.1038/nrclinonc.2014.102

Dehghani SM, Taghavi SAR, Eshraghian A, et al., 2007. Hyperlipidemia in Iranian liver transplant recipients: prevalence and risk factors. *J Gastroenterol*, 42(9):769-774. https://doi.org/10.1007/s00535-007-2092-2

Fisher FM, Maratos-Flier E, 2016. Understanding the physiology of FGF21. *Annu Rev Physiol*, 78:223-241. https://doi.org/10.1146/annurev-physiol-021115-105339

Geng LL, Lam KSL, Xu AM, 2020. The therapeutic potential of FGF21 in metabolic diseases: from bench to clinic. *Nat Rev Endocrinol*, 16(11):654-667. https://doi.org/10.1038/s41574-020-0386-0

Hondares E, Iglesias R, Giralt A, et al., 2011. Thermogenic activation induces FGF21 expression and release in brown adipose tissue. *J Biol Chem*, 286(15):12983-12990. https://doi.org/10.1074/jbc.M110.215889

Inagaki T, Dutchak P, Zhao GX, et al., 2007. Endocrine regulation of the fasting response by PPARα-mediated induction of fibroblast growth factor 21. *Cell Metab*, 5(6):415-425. https://doi.org/10.1016/j.cmet.2007.05.003

Klionsky DJ, Abdel-Aziz AK, Abdelfatah S, et al., 2021. Guidelines for the use and interpretation of assays for monitoring autophagy (4th edition). *Autophagy*, 17(1):1-382. https://doi.org/10.1080/15548627.2020.1797280

Kurosu H, Choi M, Ogawa Y, et al., 2007. Tissue-specific expression of βKlotho and fibroblast growth factor (FGF) receptor isoforms determines metabolic activity of FGF19 and FGF21. *J Biol Chem*, 282(37):26687-26695. https://doi.org/10.1074/jbc.M704165200

Li Z, Miao ZY, Ding LL, et al., 2021. Energy metabolism disorder mediated ammonia gas-induced autophagy via AMPK/mTOR/ULK1-Beclin1 pathway in chicken livers. *Ecotoxicol Environ Saf*, 217:112219. https://doi.org/10.1016/j.ecoenv.2021.112219

Ling Q, Huang HT, Han YQ, et al., 2020. The tacrolimus-induced glucose homeostasis imbalance in terms of the liver: from bench to bedside. *Am J Transplant*, 20(3):701-713. https://doi.org/10.1111/ajt.15665

Liu KP, Qiu DB, Liang X, et al., 2022. Lipotoxicity-induced STING1 activation stimulates MTORC1 and restricts hepatic lipophagy. *Autophagy*, 18(4):860-876. https://doi.org/10.1080/15548627.2021.1961072

Liu LH, Tao ZP, Zheng LD, et al., 2016. FoxO1 interacts with transcription factor EB and differentially regulates mitochondrial uncoupling proteins via autophagy in adipocytes. *Cell Death Discov*, 2:16066. https://doi.org/10.1038/cddiscovery.2016.66

Markan KR, Naber MC, Ameka MK, et al., 2014. Circulating FGF21 is liver derived and enhances glucose uptake during refeeding and overfeeding. *Diabetes*, 63(12):4057-4063. https://doi.org/10.2337/db14-0595

Medina DL, 2021. Lysosomal calcium and autophagy. *Int Rev Cell Mol Biol*, 362:141-170. https://doi.org/10.1016/bs.ircmb.2021.03.002

Nezich CL, Wang CX, Fogel AI, et al., 2015. MiT/TFE transcription factors are activated during mitophagy downstream of Parkin and Atg5. *J Cell Biol*, 210(3):435-450. https://doi.org/10.1083/jcb.201501002

Pereira MJ, Palming J, Rizell M, et al., 2013. The immunosuppressive agents rapamycin, cyclosporin A and tacrolimus increase lipolysis, inhibit lipid storage and alter expression of genes involved in lipid metabolism in human adipose tissue. *Mol Cell Endocrinol*, 365(2):260-269. https://doi.org/10.1016/j.mce.2012.10.030

Qiang WD, Shen TZ, Noman M, et al., 2021. Fibroblast growth factor 21 augments autophagy and reduces apoptosis in damaged liver to improve tissue regeneration in zebrafish. *Front Cell Dev Biol*, 9:756743. https://doi.org/10.3389/fcell.2021.756743

Qin H, Song ZY, Zhao CY, et al., 2022. Liquiritigenin inhibits lipid accumulation in 3T3-L1 cells via mTOR-mediated regulation of the autophagy mechanism. *Nutrients*, 14(6):1287. https://doi.org/10.3390/NU14061287

Rostaing L, Sánchez-Fructuoso A, Franco A, et al., 2012. Conversion to tacrolimus once-daily from ciclosporin in stable kidney transplant recipients: a multicenter study. *Transpl Int*, 25(4):391-400. https://doi.org/10.1111/j.1432-2277.2011.01409.x

Ryan A, Heath S, Cook P, 2018. Dyslipidaemia and cardiovascular risk. *BMJ*, 360:k835. https://doi.org/10.1136/bmj.k835

Settembre C, di Malta C, Polito VA, et al., 2011. TFEB links autophagy to lysosomal biogenesis. *Science*, 332(6036):1429-1433. https://doi.org/10.1126/science.1204592

She QY, Bao JF, Wang HZ, et al., 2022. Fibroblast growth factor 21: a "rheostat" for metabolic regulation? *Metabolism*, 130:155166. https://doi.org/10.1016/j.metabol.2022.155166

Sui Y, Chen JP, 2022. Hepatic FGF21: its emerging role in interorgan crosstalk and cancers. *Int J Biol Sci*, 18(15):5928-5942. https://doi.org/10.7150/ijbs.76924

Tao ZP, Aslam H, Parke J, et al., 2022. Mechanisms of autophagic responses to altered nutritional status. *J Nutr Biochem*, 103:108955. https://doi.org/10.1016/j.jnutbio.2022.108955

Veroux M, Tallarita T, Corona D, et al., 2011. Sirolimus in solid organ transplantation: current therapies and new frontiers. *Immunotherapy*, 3(12):1487-1497. https://doi.org/10.2217/imt.11.143

Visvikis O, Ihuegbu N, Labed S, et al., 2014. Innate host defense requires TFEB-mediated transcription of cytoprotective and antimicrobial genes. *Immunity*, 40(6):896-909. https://doi.org/10.1016/j.immuni.2014.05.002

Wang SY, Li HY, Yuan MH, et al., 2022. Role of AMPK in autophagy. *Front Physiol*, 13:1015500. https://doi.org/10.3389/fphys.2022.1015500

Wang YH, Wang YL, Li F, et al., 2022. Psoralen suppresses lipid deposition by alleviating insulin resistance and promoting autophagy in oleate-induced L02 cells. *Cells*, 11(7):1067. https://doi.org/10.3390/CELLS11071067

Wu AM, Feng B, Yu J, et al., 2021. Fibroblast growth factor 21 attenuates iron overload-induced liver injury and fibrosis by inhibiting ferroptosis. *Redox Biol*, 46:102131. https://doi.org/10.1016/j.redox.2021.102131

Yan LS, Zhang SF, Luo G, et al., 2022. Schisandrin B mitigates hepatic steatosis and promotes fatty acid oxidation by inducing autophagy through AMPK/mTOR signaling pathway. *Metabolism*, 131:155200. https://doi.org/10.1016/j.metabol.2022.155200

Zhang CZ, Chen KC, Wei RL, et al., 2020. The circFASN/miR-33a pathway participates in tacrolimus-induced dysregulation of hepatic triglyceride homeostasis. *Signal Transduct Target Ther*, 5:23. https://doi.org/10.1038/s41392-020-0105-2

Zhang T, Liu JX, Shen SN, et al., 2020. SIRT3 promotes lipophagy and chaperon-mediated autophagy to protect hepatocytes against lipotoxicity. *Cell Death Differ*, 27(1):329-344. https://doi.org/10.1038/s41418-019-0356-z

Supplementary information

Table S1; Figs. S1 and S2